

1 Lessons learned from the modern monsoon applied to interpretation of paleoclimate
2 records

3
4 Katherine E. Dayem^{a*}, David S. Battisti^b, Gerard H. Roe^c, Peter Molnar^d

5
6 a. Department of Geological Sciences and Cooperative Institute for Research in
7 Environmental Sciences (CIRES), University of Colorado, Campus Box 399, Boulder,
8 Colorado 80309, USA. dayem@colorado.edu, phone: +1 (303) 492-7296, fax: +1 (303)
9 492-2606

10 b. Department of Atmospheric Sciences, University of Washington, Box 351640, Seattle,
11 Washington 98195, USA. battisti@u.washington.edu

12 c. Department of Earth and Space Sciences, University of Washington, Box 351310,
13 Seattle, Washington 98195, USA. gerard@ess.washington.edu

14 d. Department of Geological Sciences and Cooperative Institute for Research in
15 Environmental Sciences (CIRES), University of Colorado, Campus Box 399, Boulder,
16 Colorado 80309, USA. molnar@colorado.edu

17
18 * corresponding author

19
20
21
22 Abstract

23 Variability in oxygen isotope ratios collected from speleothems in Chinese caves
24 are often interpreted as proxies for variability of precipitation and related to strengthening
25 and weakening of the southeast Asian monsoon, and, in some cases, the Indian monsoon.
26 Using modern data to evaluate the validity of these interpretations, we find that annual
27 and rainy season precipitation totals in each of central China, south China, and east India
28 do not correlate well with those in the other areas. The short distances over which
29 observed precipitation amounts correlate with one another does not support, though also
30 cannot by itself refute, the idea that apparently synchronous variations in $\delta^{18}\text{O}$ values at
31 widely spaced caves in China show variations in monsoon strength. We also evaluate
32 connections between climate variables and $\delta^{18}\text{O}$ values using available instrumental
33 measurements of $\delta^{18}\text{O}$ values in precipitation. These data, from stations in the Global
34 Network of Isotopes in Precipitation (GNIP), show that monthly $\delta^{18}\text{O}$ values generally do

35 not correlate well with either local precipitation or local temperature, and the degree to
36 which monthly $\delta^{18}\text{O}$ values do correlate with precipitation or temperature varies from
37 station to station. Cave speleothems, however, may record interannual, rather than
38 monthly, variations in climate, but station records of $\delta^{18}\text{O}$ values in precipitation are not
39 sufficiently long to establish whether significant correlations exist between average $\delta^{18}\text{O}$
40 values and either temperature or amount of precipitation. In the few locations that do
41 show significant correlations between $\delta^{18}\text{O}$ values and precipitation amount, we estimate
42 the change in precipitation required to account for variability in $\delta^{18}\text{O}$ values in
43 speleothems from Hulu and Dongge caves if $\delta^{18}\text{O}$ values are controlled by the
44 precipitation amount effect. We find that differences on the order of at least 50% in
45 mean annual precipitation are required to explain the $\delta^{18}\text{O}$ variations on orbital time
46 scale, which is implausibly large and inconsistent with prior GCM results. Thus, we
47 conclude that variations in $\delta^{18}\text{O}$ values in Chinese cave speleothems primarily reflect
48 changing source regions of the precipitation or changing pathways between the moisture
49 source and the paleorecord site.

50

51 Keywords: monsoon; paleoclimate; oxygen isotope ratios; Asia; precipitation; amount
52 effect

53 1. Introduction

54 To infer climate conditions in the past from a paleoclimate record, one typically
55 assumes that the primary signal in the record represents a single climate variable such as
56 precipitation amount or temperature. Oxygen isotope records obtained from cave
57 speleothems in China, for example, are usually used as a proxy for precipitation amount,
58 or ‘monsoon strength’ (e.g., Cai et al., 2006; Cheng et al., 2006; Dykoski et al., 2005;
59 Wang et al., 2008; Yuan et al., 2004). Apparent correlations between $\delta^{18}\text{O}$ records at
60 sites on the order of 1000 km apart are used to infer that changes in the isotopic records
61 are indicative of regional climate changes, which, in the case of the China records, is
62 interpreted as strengthening and weakening of the East Asian monsoon.

63 Variability of oxygen isotope ratios (expressed as $\delta^{18}\text{O}$ values) on orbital time
64 scales at three caves in China is $\sim 5\text{‰}$ at Hulu cave (32.5°N , 119.1°E) (Yuan et al.,
65 2004), ~ 5 to 6‰ at Dongge cave (25.3°N , 108.1°E) (Wang et al., 2001), and $\sim 4\text{‰}$ at
66 Xiaobailong cave (24.2°N , 103.3°E) (Cai et al., 2006) (Fig. 1). In comparison, modern
67 $\delta^{18}\text{O}$ values of precipitation obtained from Global Network of Isotopes in Precipitation
68 (GNIP) stations (IAEA/WMO, 2004) in eastern China show seasonal ranges ~ 6 to 10‰
69 (Fig. 1), and differences in mean-annual values of ~ 2 to 4‰ . Because the magnitudes of
70 variation in $\delta^{18}\text{O}$ values in the modern seasonal data and the paleorecords are similar, we
71 use the modern data to examine spatial and temporal correlations between $\delta^{18}\text{O}$ values
72 and two variables that are related to ‘monsoon strength’: precipitation and temperature.

73 The appeal of isotope ratios as proxies for precipitation or temperature is
74 understandable. To reduce a paleoclimate signal to the variability of one climate variable
75 allows a straightforward interpretation. Modern and presumably past climates, however,

76 are not so simple; isotope ratios depend on the temperature, precipitation rate, and
77 horizontal and vertical distance from the moisture source. They are also a function of the
78 moisture recycling on the continents (e.g., Gat, 1996), precipitation rate and raindrop size
79 (e.g., Lee and Fung, 2008), and the atmospheric circulation – the agent that transports
80 moisture from source to precipitation site (e.g., Dansgaard, 1964; Lee et al., 2007;
81 Rozanski et al., 1992). In essence, to understand the variability of an oxygen isotope
82 ratio signal we need to know how atmospheric processes affect isotopic ratios in
83 precipitation, and which of these processes have the largest influence on the isotope
84 signal.

85 Oxygen isotope ratios recorded in cave speleothems are also affected by processes
86 that occur between the time when the precipitation reaches the ground and when the
87 oxygen atoms are incorporated in the speleothem. For example, retention of water in the
88 soil may serve to average $\delta^{18}\text{O}$ values over several years (Vaks et al., 2003), and variation
89 of cave temperature (Johnson et al., 2006a) may lead to variation in fractionation during
90 the speleothem formation process. Vegetation and aquifer conditions may also affect
91 speleothem formation (Fairchild et al., 2006). Thus, our ability to demonstrate that a
92 paleoclimate record is a signal of atmospheric processes and to interpret that record
93 depends on an understanding of the hydrology of the cave and the aquifer above it (e.g.,
94 Fairchild et al., 2006).

95 To our knowledge, there has been only one study of the isotopic composition of
96 dripwater in any Chinese cave to assess the degree to which fractionation and mixing
97 may occur on the oxygen's path from precipitation to speleothem. Johnson et al. (2006a)
98 study monthly resolved data from a stalagmite from Heshang Cave (30.4°N, 110.4°E),

99 which lies ~ 600 km northeast of Dongge and ~ 1000 km southwest of Hulu, two caves
100 where long times series of $\delta^{18}\text{O}$ values have been derived from speleothems. Johnson et
101 al. (2006a) find that both precipitation and temperature influence $\delta^{18}\text{O}$ values in cave drip
102 water and speleothems on a monthly to yearly timescale. At the opposite extreme, the
103 continuous sampling method used to sample the speleothem along its growth axis may
104 average out any time resolution shorter than several years to hundreds of years (e.g., Cai
105 et al., 2006; Cheng et al., 2006; Hu et al., 2008; Yuan et al., 2004).

106 In summary, many processes in both the atmosphere and the aquifer influence
107 $\delta^{18}\text{O}$ values in cave speleothems. In a step toward understanding what such values imply
108 for paleoclimate, we focus on two questions regarding interpretation of these records:
109 How large an area does a paleorecord describe? and: Can we demonstrate that
110 precipitation amount (or monsoon strength) is the primary influence on these $\delta^{18}\text{O}$
111 values? To answer the former, we examine the spatial extent of correlations of
112 precipitation and temperature of cave locations with the rest of Asia. To answer the latter
113 question, we test for correlation between $\delta^{18}\text{O}$ values and precipitation or temperature,
114 and we estimate precipitation in the past assuming that precipitation amount is the main
115 influence on $\delta^{18}\text{O}$ values. Although the magnitude of seasonal and interannual variation
116 in modern data is comparable to the difference between high and low values of $\delta^{18}\text{O}$
117 recorded in cave speleothems, we do recognize that the time scales that we consider may
118 be too short to allow us to examine all processes that affect $\delta^{18}\text{O}$ values, and that other
119 tools, such as GCM experiments, may be required for paleoclimatic interpretation of such
120 records.

121

122 2. Spatial extent of variability

123 The paucity of paleoclimate records and the large investments in time and money
124 required to obtain them make it appealing to apply climatic inferences from a given
125 record to as large an area as possible. Authors of studies of this nature typically apply
126 interpretations to the entire East Asian monsoon region (e.g., Cheng et al., 2006; Kelly et
127 al., 2006; Wang et al., 2008; Yuan et al., 2004), and some strive to link the East Asian
128 monsoon to the Indian monsoon (e.g., Cai et al., 2006). In this section we establish that
129 variability in modern data do not support this generalization, at least on interannual to
130 decadal timescales.

131 Regions impacted by monsoon precipitation, such as northern India and southeast
132 China, receive large amounts of precipitation, even in the annual mean (Fig. 2). We test
133 whether variations in annual precipitation are similar across these broad monsoon
134 impacted regions in China and India by correlating annual mean precipitation and
135 temperature from the NCAR/NCEP reanalysis data set (e.g., Kalnay et al., 1996) at sites
136 near Hulu, Dongge, and Dandak (East India) caves, where $\delta^{18}\text{O}$ records have been
137 collected from cave speleothems (Sinha et al., 2007; Wang et al., 2001; Yuan et al.,
138 2004), with the same variables at all other points in Asia. We carried out the same
139 correlations using data from the ECMWF ERA-40 data set, and found patterns similar to
140 those we describe below. Annual (January to December) mean precipitation, which
141 eliminates the seasonal march in precipitation from south to north in eastern China,
142 correlates positively and significantly over relatively small spatial scales (Fig. 3, left
143 column). The spatial scale of significant correlation is ~ 500 km near Hulu cave and
144 slightly near larger Dongge cave (Fig. 3c). Thus, a strong monsoon near one cave does

145 not imply a strong monsoon at another. Precipitation on the east coast of India correlates
146 with precipitation over the whole of northern India, but hardly at all with anywhere in
147 China (Fig. 3e). The lack of significant correlation between precipitation near Hulu cave
148 with either Dongge cave or East India, and none between the latter two sites either,
149 suggests that the Indian and southeast Asian monsoon systems are broadly separate (e.g.,
150 Fasullo and Webster, 2003; Maher, 2008; Wang and Fan, 1999; Webster et al., 1998),
151 and that the processes that affect monsoon variability in eastern China seem to behave
152 differently in the north and south (e.g., Lee et al., 2008).

153 Mean annual temperature covaries over a broader region than does precipitation
154 (Fig. 3, right column). The temperature near Hulu cave correlates positively and
155 significantly with temperature along eastern China and north of the Tibetan plateau (Fig.
156 3b). Temperature near Dongge cave covaries with temperature in southern China,
157 northern India, and north of the Tibetan plateau (Fig. 3d). Temperature in eastern India
158 correlates positively with that across India and southeastern Asia (Fig. 3f). Correlations
159 made using rainy season mean temperature show similar patterns. Thus, a paleorecord
160 that is assumed to be a proxy for temperature may describe a larger region than one
161 assumed to be a proxy for precipitation. If variability of $\delta^{18}\text{O}$ values at Hulu and Dongge
162 caves were the response to variability in temperature, the positive correlation seen in the
163 orbital time-scale variability in $\delta^{18}\text{O}$ values in these two places would be consistent with
164 variability in modern climate.

165 Although we do not obtain significant correlations over a broad area for
166 precipitation, it does not necessarily follow that that wide-spread covariance in
167 precipitation did not occur in the past climates, which responded to different insolation

168 forcing than modern climate. The degree of spatial covariance in precipitation might be
169 tested using GCM simulations for past climates such as those made for paleoclimate
170 modeling intercomparison project (PMIP) (Joussaume and Taylor, 1995), which, to our
171 knowledge, has not been published.

172

173 3. Seasonality of modern precipitation and temperature

174 The seasonality of climate in India is characterized by wet summers associated
175 with the Indian monsoon and relatively dry winters. Moisture that falls as summertime
176 monsoon precipitation in India is transported from the Bay of Bengal by a succession of
177 storms, known as Bengali depressions (e.g., Gadgil, 2003). These may result from
178 differential heating between Asia and the Indian Ocean, or from movement of the
179 intertropical convergence zone (ITCZ) over the region (Gadgil, 2003).

180 In contrast, seasonality of present-day precipitation in eastern China varies from
181 south to north (Fig. 1). Precipitation rates are maximum in the spring in southeast China
182 (see stations Guilin, Hong Kong, Liuzhou, and to a lesser degree Fuzhou in Fig. 1), but
183 are maximum in mid- to late summer farther north (see Nanjing and Shijiazhuang, Fig.
184 1). This south to north progression of high precipitation rates follows the path of the
185 Meiyu front, a warm, humid, and convective subtropical frontal system that is related to
186 the subtropical high-pressure system over the western Pacific Ocean (Zhou et al., 2004
187 and references therein). The front stretches northeast to southwest over southeast China,
188 extends as far west as $\sim 105^{\circ}\text{E}$ and as far north $\sim 35^{\circ}\text{N}$ (Zhou et al., 2004) (Fig. 1). Only
189 two of the stations we examine lie outside the Meiyu front region: Shijiazhuang is north
190 of the northernmost location of the front, and Kunming is west of the region affected by

191 frontal dynamics (Fig. 1). Stations at Guiyang and Zunyi are on the western edge of the
192 Meiyu front region, and receive maximum precipitation rates in the early summer rather
193 than in the spring due to the NE-SW orientation of the front (Fig. 1). Winds associated
194 with Meiyu frontal precipitation are generally from the south.

195 Thus the term ‘monsoon’ applied to southeast China region is somewhat
196 misleading; the majority of the precipitation that falls in southeast China results from
197 frontal dynamics rather than differential land-sea heating or the northward progression of
198 the ITCZ. Coastal stations Hong Kong and Fuzhou receive high precipitation rates again
199 in the summer after the Meiyu front has moved northward. These high precipitation rates
200 are associated with easterly winds (not shown) and may be a result of local differential
201 land-sea heating. We stress, however, that the majority of the precipitation in southeast
202 China is associated with frontal dynamics and convergence of the large-scale circulation.

203 The difference in the seasonality of precipitation and in the atmospheric dynamics
204 that delivers it to the continent supports the lack of correlation between either
205 temperature or precipitation in southeast China with that of India in the modern climate
206 (Fig. 3). Comparisons of proxies of Indian monsoon and southeast China precipitation
207 contain the underlying assumption that in past climates, broad regions are responding to
208 some forcing in the same way, which is not supported by the analysis above.

209

210 4. Correlation of $\delta^{18}\text{O}$ values with precipitation and temperature

211 *4.1 Monthly correlations*

212 We wish to test the assumption that $\delta^{18}\text{O}$ values are controlled either by the
213 amount of precipitation or by local temperature. To do so, we use data from GNIP

214 stations (IAEA/WMO, 2004) in eastern China (Fig. 1) to calculate correlations for
215 monthly and for 12-month and 24-month running average values of $\delta^{18}\text{O}$, temperature,
216 and precipitation. Although modern $\delta^{18}\text{O}$ data is limited to as few as 5 years at some
217 stations with a maximum of 35 years at Hong Kong, we expect that if robust relationships
218 between $\delta^{18}\text{O}$ values and precipitation or temperature exist, even these short term modern
219 records should show systematic correlations with climate variables. Correlations on the
220 monthly time scale contain information on present-day atmospheric variability.
221 Correlations using one- or two-year running average data may better reflect the
222 atmospheric variability as it is recorded in cave speleothem records, as the latter reflects a
223 smoothed version of $\delta^{18}\text{O}$ values in precipitation due to the retention time in the soil
224 above a cave (e.g., Johnson et al., 2006a; Vaks et al., 2003). We also report correlations
225 between anomalies (differences between monthly values and the corresponding average
226 monthly value) of the same variables, to remove correlations associated with the seasonal
227 cycle. In the remainder of this section, we show that where significant correlations exist,
228 monthly correlations between $\delta^{18}\text{O}$ values and temperature or precipitation vary from
229 station to station and explain < 50 % of the variance in all cases. In general, temperature
230 is better anticorrelated with $\delta^{18}\text{O}$ values than is precipitation. Correlations between 12-
231 and 24-month running averages of the variables are generally not significant, leading us
232 to urge caution to those who assume that $\delta^{18}\text{O}$ values in speleothems are a proxy for the
233 amount of climatological precipitation.

234 On a seasonal cycle, temperature and $\delta^{18}\text{O}$ values covary (anti-phased) at most
235 sites. Temperature is maximum in summer and $\delta^{18}\text{O}$ values are smallest in the late
236 summer to early fall (Fig. 1). Values of $\delta^{18}\text{O}$ are generally less negative in the

237 wintertime. Precipitation does not covary with $\delta^{18}\text{O}$ values throughout southern China,
238 where maximum precipitation occurs in springtime, and $\delta^{18}\text{O}$ values reach a minimum in
239 late summer (Fig. 1).

240 For the few stations that show a statistically significant relationship, monthly
241 correlations between $\delta^{18}\text{O}$ values and precipitation amount are negative (Table 1). Plots
242 of $\delta^{18}\text{O}$ values versus monthly precipitation (Fig. 4) indeed show large scatter at most
243 sites. Correlations statistically significant from zero are found only at Guiyang, Hong
244 Kong, Kunming, and Zunyi. Correlation coefficients between monthly anomalies of $\delta^{18}\text{O}$
245 values and monthly anomalies in precipitation are also negative, but are significantly
246 different from zero only at Hong Kong.

247 Fig. 4 shows scatter plots of the monthly averaged values of $\delta^{18}\text{O}$ versus
248 temperature for all stations. Where correlations are significant (see Table 1), temperature
249 is negatively correlated with $\delta^{18}\text{O}$, except at Shijiazhuang, which lies north of the Meiyu
250 front region and is unaffected by monsoon precipitation (Fig. 1). In contrast, monthly
251 anomalies of $\delta^{18}\text{O}$ values and temperature are positively correlated where the correlation
252 is significant, at Kunming and Shijiazhuang, the two stations unaffected by the Meiyu
253 front. These differences between correlations of raw monthly data and those with the
254 seasonal cycle removed suggest that the seasonal cycle contains much of the information
255 in the $\delta^{18}\text{O}$ signal. Thus we suspect that the correlations between $\delta^{18}\text{O}$ values and
256 temperature result from correlations of each variable with some other seasonally varying
257 variable such as insolation or the large-scale atmospheric circulation. If this is the case, it
258 need not be local temperature that determines $\delta^{18}\text{O}$ values, but instead some other
259 independent process that affects both temperature and the value of the $\delta^{18}\text{O}$ in the

260 precipitation. Local temperature is thus an indicator of – not the cause of – changes in
261 processes elsewhere and the latter determine the $\delta^{18}\text{O}$ that is being precipitated over
262 China. We also note that just as $\delta^{18}\text{O}$ values in the paleorecords decrease with summer
263 insolation and hence presumably increasing local temperature (Cai et al., 2006; Wang et
264 al., 2001; Yuan et al., 2004), modern $\delta^{18}\text{O}$ values decrease with increasing temperature,
265 which is opposite the prediction from Rayleigh fractionation that $\delta^{18}\text{O}$ values increase
266 with increasing temperature (e.g., Dansgaard, 1964). The lack of agreement between
267 trends in modern $\delta^{18}\text{O}$ values and Rayleigh fractionation has been observed globally in
268 both observations and model results (e.g., Brown et al., 2008; Lee et al., 2007), and
269 suggests that if temperature influences $\delta^{18}\text{O}$ values, then Rayleigh fractionation is not the
270 dominant process by which that occurs.

271 All sites in our study receive most of their precipitation in the spring and/or
272 summer seasons, which means that monthly average temperature and precipitation are
273 positively correlated. To test whether the lack of independence between precipitation and
274 temperature affects the correlations above, we calculate partial correlation coefficients for
275 the monthly mean time series, which remove the influence of either temperature or
276 precipitation (e.g., Arkin and Colton, 1970). For example, the partial correlation
277 $\rho(\delta^{18}\text{O}, T, P)$ is the correlation between $\delta^{18}\text{O}$ values and temperature with the effect of the
278 correlation between temperature and precipitation removed. Where significant, partial
279 correlation coefficients have the same sign and tend to be slightly smaller in magnitude
280 than the correlation coefficients (Table 1), suggesting that correlation between
281 temperature and precipitation affects correlations between $\delta^{18}\text{O}$ values and temperature or
282 precipitation by only a small amount.

283

284 *4.2 Interannual correlations*

285 For comparison to paleoclimate records, correlations between longer time
286 intervals may be more appropriate. Therefore we calculate correlations between 12-
287 month and 24-month running average values of $\delta^{18}\text{O}$ with corresponding averages of
288 precipitation and temperature. Note that in calculating 12- and 24-month averages of
289 $\delta^{18}\text{O}$ values, we use the monthly values of $\delta^{18}\text{O}$ weighed by the amount of the
290 precipitation that fell that month and denoted by $\delta^{18}\text{O}_w$. To assess statistical significance,
291 we use an effective degrees of freedom $n - 2$ where n is the number of years of data for
292 12-month averages and half that number for 24-month averages. Because of the limited
293 amount of data available, no correlations are significant at the 95% confidence level.
294 Only the correlations between 12- and 24-month running average values of $\delta^{18}\text{O}_w$ and
295 temperature at Hong Kong are significant at the 80 % confidence level ($r = -0.30$ (12-
296 month average), $r = -0.45$ (24-month average)), which is suggestive at best. Thus the
297 available instrumental observations provide evidence that neither supports nor denies the
298 normal paleoclimate interpretation. Beyond waiting for longer timeseries of isotope
299 measurements to become available, another approach to build confidence in the correct
300 climatic interpretation of the speleothem record may be climate model studies that test
301 how $\delta^{18}\text{O}$ values in precipitation respond to various atmospheric processes (e.g., Bony et
302 al., 2008; Lee et al., 2007; Lee and Fung, 2008; Risi et al., 2008).

303 Although the statistics do not allow for definitive conclusions to be made, they
304 are suggestive of correlations that are consistent with the global scale findings of
305 Rozanski et al. (1992). They find that anomalies of 12-month average $\delta^{18}\text{O}$ values are

306 positively correlated with temperature at mid-latitudes, but that there is little relationship
307 between the either temperature or precipitation at Hong Kong, which is consistent with
308 results from other tropical regions that they examined and are affected by a monsoon.
309 The two coastal sites that receive both springtime precipitation related to the Meiyu front
310 dynamics and summertime precipitation presumably related to typical monsoon
311 differential heating (Hong Kong and Fuzhou) may fit with Rozanski et al.'s (1992)
312 tropical sites, and inland sites may fit with their mid-latitude sites.

313

314 5. Discussion

315 Monthly correlations suggest that variations in $\delta^{18}\text{O}$ values generally correlate
316 better with temperature than with precipitation. At all stations except Shijiazhuang, $\delta^{18}\text{O}$
317 values are negatively correlated with temperature, so that rainwater is isotopically lighter
318 when temperature is higher (summer). This is the same sign sense as the orbitally
319 induced changes in paleoclimate records: $\delta^{18}\text{O}$ values are more depleted during warmer
320 times (e.g., Cai et al., 2006; Wang et al., 2001; Yuan et al., 2004), but opposite to that
321 predicted by Rayleigh fractionation: $\delta^{18}\text{O}$ values increase with temperature (e.g.,
322 Dansgaard, 1964). For northern and western stations (Guiyang, Kunming, Nanjing,
323 Shijiazhuang, and Zunyi), maximum temperature and depleted $\delta^{18}\text{O}$ values also
324 correspond to the maximum precipitation rate (Fig. 1). Locations in southeast China such
325 as Guilin and Liuzhou, however, receive their maximum precipitation rates in the
326 springtime. Minimum $\delta^{18}\text{O}$ values and maximum temperature occur in the summer at the
327 southeast China sites, and $\delta^{18}\text{O}$ is more negatively correlated to temperature than
328 precipitation. Because correlations between monthly anomalies of $\delta^{18}\text{O}$ values and

329 precipitation or temperature are small and, with a few exceptions, insignificant, we infer
330 that much of the variation in $\delta^{18}\text{O}$ values results from seasonal variation of some process
331 and does not reflect local temperature or precipitation.

332 Johnson and Ingram (2004) perform multiple regression analyses on 3 years of
333 data from most of the same GNIP stations in China. They deduce that $\delta^{18}\text{O}$ values are
334 influenced primarily by precipitation in areas that are affected by the summer monsoon,
335 and by temperature in areas not affected by the summer monsoon. Although partial
336 correlation coefficients (Table 1) do support their conclusion that precipitation
337 contributes to the $\delta^{18}\text{O}$ signal in Hong Kong (which is influenced by the summer
338 monsoon), and to some extent at Shijiazhuang, which is north of the monsoon region
339 (Fig. 1; Table 1). At these and other sites, however, the partial correlation coefficients
340 relating monthly values of $\delta^{18}\text{O}$ to temperature are larger in magnitude than those for
341 precipitation (Table 1). Thus, if cave records provide information on a monthly scale,
342 our results from the modern day climate imply that the $\delta^{18}\text{O}$ signal in cave records from
343 central China is indicative of non-local changes (such as changes in source regions of the
344 precipitating water, changes in the source or pathway between moisture source and the
345 precipitating site) that on orbital time scales are due to changes in insolation which also
346 causes temperature changes over China that are passively correlated with co-located $\delta^{18}\text{O}$
347 values.

348 Cave speleothems do not appear to record monthly variations in precipitation.
349 Precipitated water may be retained and mixed in the soil layer for one or more years
350 before it seeps into a cave (e.g., Vaks et al., 2003). Consequently an understanding of 12-
351 month or 24-month running averages of modern station data would be ideal to interpret

352 paleoclimate records from cave speleothems. Unfortunately, station records are not long
353 enough to obtain significant results with the exception of the Hong Kong record, which
354 suggests that $\delta^{18}\text{O}_w$ values and temperature are negatively correlated. In general, there is
355 insufficient data available to provide support for the claim that the $\delta^{18}\text{O}_w$ record obtained
356 from a cave stalagmite is a simple a proxy for monsoon strength.

357 We can, however, perform a scale analysis to explore whether it is plausible for
358 local precipitation changes to explain the orbital time scale changes in $\delta^{18}\text{O}$ in the cave
359 records. For the sake of argument, let us assume that $\delta^{18}\text{O}$ values are a valid proxy for
360 precipitation, and ask: How much must annual precipitation change to produce the
361 amplitude of $\delta^{18}\text{O}$ values in the paleorecords? The maximum amplitude of the orbital
362 timescale swings of $\delta^{18}\text{O}$ values from Dongge cave is $\sim 4 - 5 \text{‰}$ at $\sim 130 \text{ ka}$ (Yuan et al.,
363 2004). The amplitude of variability in modern $\delta^{18}\text{O}$ values is $\sim 7 - 8 \text{‰}$, and for
364 comparison the most recent minimum $\delta^{18}\text{O}$ value is $\sim -9 \text{‰}$ at $\sim 9 \text{ ka}$ and the most recent
365 maximum $\delta^{18}\text{O}$ value is $\sim -5 \text{‰}$ at $\sim 15\text{ka}$ (Yuan et al., 2004).

366 We estimate weighted annual $\delta^{18}\text{O}$ values for hypothetical past climates with
367 mean annual precipitation and seasonal amplitudes different from those day. We write
368 monthly precipitation as the sum of the annual average plus the monthly anomaly:

369
$$P(t) = f_o P_o + f' P'(t) \quad (1)$$

370 where f_o and f' are weights on the annual mean and amplitude of seasonal variability,
371 respectively. For the modern day, $f_o = f' = 1$. For a climate where mean annual
372 precipitation is larger (smaller) than present, $f_o > 1$ ($f_o < 1$). For a climate with wetter

373 summers and drier winters (stronger monsoon) than present, $f' > 1$, and for a climate with
374 less seasonal variability (less monsoonal) than present, $f' < 1$.

375 We want to test the effect of varying the annual mean with f_o and the seasonal
376 amplitude with f' , assuming that $\delta^{18}\text{O}$ values are controlled by the amount of
377 precipitation. We determine empirical relationships between monthly precipitation and
378 monthly average $\delta^{18}\text{O}$ values for each station using the station data. We fit $\delta^{18}\text{O}$ values
379 as a function of precipitation (Fig. 4) with straight lines, and use those lines to define the
380 relationship between $\delta^{18}\text{O}$ values and precipitation:

$$\begin{aligned} \delta_o &= aP_o + b \\ \delta'(t) &= aP'(t) \end{aligned} \quad (2)$$

382 where $a = \Delta\delta^{18}\text{O}/\Delta P$ is the slope of the best fit line and b is its y-intercept. Admittedly,
383 this method is crude – the modern data shows so much scatter that a linear fit may not be
384 reasonable (Fig. 4), but we proceed nonetheless and consider stations where monthly
385 values of $\delta^{18}\text{O}$ and precipitation are significantly correlated: Guiyang, Hong Kong,
386 Kunming, and Zunyi, noting that others have used linear regressions to estimate changes
387 in precipitation inferred from $\delta^{18}\text{O}$ records. For example, Johnson et al. (2006b) deduce
388 that an 80% decrease in precipitation is needed to explain a 3 ‰ reduction in $\delta^{18}\text{O}$ values
389 in a record from Wanxiang Cave, which is north of the northern limit of the Meiyu front,
390 and they too go on to argue that the $\delta^{18}\text{O}$ record at this cave cannot be accounted for by
391 the amount effect or by changes in temperature.

392 Assuming the seasonal cycle can be described with a cosine function,

$$P'(t) = P_a \cos(t) \quad (3)$$

394 where P_a is the maximum precipitation anomaly, the $\delta^{18}\text{O}$ value adjusted for this
 395 approximation to the amount effect is then:

$$396 \quad \delta_{ae}(t) = \frac{\int_0^{2\pi} P \delta dt}{\int_0^{2\pi} P dt}. \quad (4)$$

397 Using (1) and (2) to substitute for $P(t)$ and δ_o and integrating yields:

$$398 \quad \delta_{ae} = af_o P_o + b + \frac{af'^2 P_a^2}{2f_o P_o} \quad (5)$$

399 Then the difference between a past climate state and the modern is:

$$400 \quad D = aP_o \left[(f_o - 1) + \frac{1}{2} \left(\frac{f'^2}{f_o} - 1 \right) \right]. \quad (6)$$

401 To simplify matters, we have assumed that $P_a = P_o$ in (6) (i.e., modern precipitation is $P =$
 402 $P_o(1 - \cos(t))$, and require that $|f'/f_o| \leq 1$ for positive values of precipitation. Note that
 403 the difference between past and modern climates is not dependent on b because we have
 404 assumed that the relationship between $\delta^{18}\text{O}$ value and precipitation is invariant with time.
 405 Using modern data to find a and P_o for each station, we plot D as a function of f_o holding
 406 $f' = 1$ (Fig. 5a) and D as a function of f' holding $f_o = 1$ (Fig. 5b). The minimum f_o and
 407 maximum f' values are limits beyond which the absolute value of the monthly
 408 precipitation anomaly in the driest months of the year is larger than the annual mean,
 409 resulting in negative precipitation for the month. We also calculated D using the modern
 410 day seasonal cycle instead of a cosine function, and the resulting curves differ only
 411 slightly in shape from those plotted in Fig. 5. Thus variation in the shape of the seasonal
 412 cycle has little effect on D .

413 To decrease the $\delta^{18}\text{O}$ value by 1 ‰ (the approximate difference between $\delta^{18}\text{O}$
414 values of present-day and 9 ka), the mean annual precipitation must be ~1.5 times larger
415 than present at Kunming and Zunyi, and as much as ~2 times larger than present at Hong
416 Kong (Fig. 5a). In this formulation, changing the amplitude of the seasonal cycle cannot
417 cause a decrease of the $\delta^{18}\text{O}$ value by 1 ‰ given the upper limit of f' (Fig. 5b). Kutzbach
418 (1981) estimates ~ 10 % increase in summertime precipitation and ~ 5 % increase in
419 annually averaged precipitation amount between modern day and 9 ka using general
420 circulation model experiments. GCM ensemble results from the PMIP2 experiment show
421 no change in annual mean precipitation from 6 ka to present (Braconnot et al., 2007).
422 Our calculations above suggest that if the amount effect is responsible for the difference
423 in $\delta^{18}\text{O}$ values between the two times, the change in precipitation amount must be much
424 larger (Fig. 5a). Sustained differences of 50% or more between present-day and modern
425 annual precipitation seem unlikely, and thus this calculation suggests that insofar as the
426 modern dependence of $\delta^{18}\text{O}$ values on precipitation applies to paleoclimate, monsoon
427 strength cannot be the explanation for the large variations in $\delta^{18}\text{O}$ values in speleothems
428 in China.

429 Finally, the station-specific amount effect a calculated above is similar to that
430 calculated by Bony et al. (2008) using a simple column-integrated model over tropical
431 ocean and by Lee et al. (2008) using atmospheric GCM with an isotope model (Lee et al.,
432 2007). For a relatively modest change in $\delta^{18}\text{O}$ of 2 ‰, what is the change in precipitation
433 predicted by the models and our empirical relationship for Hong Kong (the most tropical
434 stations analyzed here)? For Hong Kong's average precipitation rate of 196 mm/month, a
435 2 ‰ change in $\delta^{18}\text{O}$ values implies a change in precipitation of ~ 68 % estimated from

436 Bony et al.'s (2008) $\delta^{18}\text{O}$ /precipitation relationship, ~ 100 % estimated from Lee et al.
437 (2007) model, and ~ 225 % from the GNIP Hong Kong data above. Such large changes
438 in precipitation are unlikely, which provides another argument against the assumption
439 that precipitation amounts are the dominant control on $\delta^{18}\text{O}$ values in instrumental or
440 paleoclimate records.

441

442 6. Conclusions

443 Although $\delta^{18}\text{O}$ values from cave records in China are often interpreted as records
444 of variations in Asian monsoon strength, modern station data offer little support for the
445 idea that variations in $\delta^{18}\text{O}$ values reflect variations in precipitation. In fact, correlations
446 between monthly data suggest that temperature variations correlate better with variations
447 in $\delta^{18}\text{O}$ values. Monthly $\delta^{18}\text{O}$ values correlate negatively with temperature – the same
448 sign of the correlation between $\delta^{18}\text{O}$ values in the cave records and the amplitude of
449 insolation ($\delta^{18}\text{O}$ values are more depleted during warmer times) – and are opposite to that
450 expected from Rayleigh fractionation ($\delta^{18}\text{O}$ values increase with temperature). Monthly
451 anomalies of $\delta^{18}\text{O}$ values, however, do not generally correlate with monthly anomalies of
452 temperature, indicating that much of the covariance between $\delta^{18}\text{O}$ values and temperature
453 is contained in the seasonal cycle. Thus we propose that variation of $\delta^{18}\text{O}$ values and
454 temperature on the seasonal time scale primarily reflect independent processes that are
455 both regulated by changes in insolation (e.g., local insolation directly regulates local
456 temperature, and global insolation gradients – correlated with local insolation – affects
457 the source regions and pathways of the $\delta^{18}\text{O}$ as it is delivered to the local site).

458 Cave speleothems, however, record a $\delta^{18}\text{O}$ signal of precipitation averaged over
459 several years because precipitation must percolate through the soil before reaching the
460 cave and being precipitated on the stalagmite. Modern station data averaged over 12 or
461 24 months do not show significant variations between $\delta^{18}\text{O}_w$ values and temperature or
462 precipitation at most stations. It is possible that such correlations do exist, but that they
463 cannot be inferred on the basis of the short duration of the observations.

464 Finally, if we assume that the $\delta^{18}\text{O}$ values from a paleoclimate record are a proxy
465 for precipitation amount, then we can make a crude estimate of the difference in
466 precipitation between present day and times in the past. Our calculations show that for a
467 $\sim 1\%$ increase in $\delta^{18}\text{O}$ values, the difference between modern and 9 ka $\delta^{18}\text{O}$ values at
468 Dongge and Hulu caves (e.g., Wang et al., 2001; Yuan et al., 2004), annual precipitation
469 9 ka would be at least 1.5 times that of today. Calculations using atmospheric general
470 circulation models estimate this difference to be much smaller, around 10%. Thus
471 paleoclimate records may not be a proxy for one single variable, but a combination of
472 atmospheric processes.

473 Though not a perfect analogue for the past, the modern instrumental record and
474 the patterns of modern climate variability offer insights on the causes of past changes in
475 environmental conditions. In the context of interpreting the records of Asian speleothems,
476 the modern record does not support the conventional paleoclimatic interpretation that
477 $\delta^{18}\text{O}$ values reflect precipitation amount. In fact, correlations between monthly data
478 suggest that temperature variations correlate better to variations $\delta^{18}\text{O}$ values, although
479 neither precipitation nor temperature explains a majority of the variance. In light of these
480 results, we suspect that other processes, such as re-evaporation, storm type, and variations

481 in atmospheric circulation have more of an influence on $\delta^{18}\text{O}$ values than do precipitation
482 or temperature.

483 Acknowledgments

484 This work was funded by the US National Science Foundation, Continental Dynamics
485 Program (EAR-0507431). NCEP Reanalysis data provided by the NOAA/OAR/ESRL
486 PSD, Boulder, Colorado, USA from their website at <http://www.cdc.noaa.gov/>. Legates
487 Surface and Ship Observation of Precipitation data was obtained from the Goddard Earth
488 Sciences Data Information and Services Center: <http://daac.gsfc.nasa.gov/precipitation/>.
489 PMIP2 data was downloaded from their project website at <http://pmip2.lsce.ipsl.fr/>.

490 References

491

492 Arkin, H., Colton, R.R., 1970. *Statistical Methods*, Harper & Row, New York.

493

494 Bony, S., Risi, C., Vimeux, F., 2008. Influence of convective processes on the isotopic
495 composition ($\delta^{18}\text{O}$ and δD) of precipitation and water vapor in the tropics: 1.
496 Radiative-convective equilibrium and the Tropical Ocean-Global Atmosphere-
497 Coupled Ocean-Atmosphere Response Experiment (TOGA-COARE) simulations,
498 *J. Geophys. Res.*, 113, 10.1029/2008JD009942.

499

500 Braconnot, P., et al., 2007. Results of PMIP2 coupled simulations of the Mid-Holocene
501 and Last Glacial Maximum – Part 1: experiments and large-scale features,
502 *Climate of the Past*, 3, 261-277.

503

504 Brown, D., Worden, J., Noone, D., 2008. Comparison of atmospheric hydrology over
505 convective continental regions using water vapor isotope measurements from
506 space, *J. Geophys. Res.*, 113, doi:10.1029/2007JD009676.

507

508 Cai, Y., An, Z., Cheng, H., Edwards, R.L., Kelly, M.J., Liu, W., Wang, X., Shen, C.-C.,
509 2006. High-resolution absolute-dated Indian Monsoon record between 53 and 36
510 ka from Xiaobailong Cave, southwestern China, *Geology*, 34, 621-624.

511

512 Cheng, H., Edwards, R.L., Wang, Y.J., Kong, X.G., Ming, Y.F., Kelly, M.J., Wang, X.F.,
513 Gallup, C.D., Liu, W.G, 2006. A penultimate glacial monsoon record from Hulu
514 Cave and two-phase glacial terminations, *Geology*, 34, 217-220.

515

516 Dansgaard, W., 1964. Stable isotopes in precipitation, *Tellus*, 16, 436-486.

517

518 Dykoski, C.A., Edwards, R.L., Cheng, H., Yuan, D., Cai, Y., Zhang, M., Lin, Y., Qing,
519 J., An, Z., Revenaugh, J., 2005. A high-resolution, absolute-dated Holocene and
520 deglacial Asian monsoon record from Dongge Cave, China, *Earth Planet. Sci.*
521 *Lett*, 233, 71-86.

522

523 Fairchild, I.J., Smith, C.L., Baker, A., Fuller, L., Spötl, C., Matthey, D., McDermott, F.,
524 E.I.M.F, 2006. Modification and preservation of environmental signals in
525 speleothems, *Earth Sci. Rev.*, 75, 105-153.

526

527 Fasullo, J., Webster, P.J., 2003. A hydrological definition of Indian Monsoon onset and
528 withdrawal, *J. Climate*, 16, 3200-3211.

529

530 Gadgil, S., 2003. The Indian monsoon and its variability, *Annu. Rev. Planet. Sci.*, 31,
531 429-467.

532

533 Gat, J.R., 1996. Oxygen and hydrogen isotopes in the hydrologic cycle, *Annu. Rev.*
534 *Earth Planet. Sci.*, 24, 225-262.

535

536 Hu, C., Henderson, G.M., Huang, J., Xie, S., Sun, Y., Johnson, K.R., 2008.
537 Quantification of Holocene Asian monsoon rainfall from spatially separated cave
538 records, *Earth Planet. Sci. Lett.*, 266, 221-232.
539

540 IAEA/WMO, 2004. Global Network of Isotopes in Precipitation, The GNIP Database.
541 Accessible at: <http://isohis.iaea.org>
542

543 Johnson, K.R., Ingram, B.L., 2004. Spatial and temporal variability in the stable isotope
544 systematics of modern precipitation in China: implications for paleoclimate
545 reconstructions, *Earth Planet. Sci. Lett.*, 220, 365-377.
546

547 Johnson, K.R., Hu, C., Belshaw, N.S., Henderson, G.M., 2006a. Seasonal trace-element
548 and stable-isotope variations in a Chinese speleothem: The potential for high-
549 resolution paleomonsoon reconstruction, *Earth Planet. Sci. Lett.*, 244, 221-232.
550

551 Johnson, K.R., Ingram, B.L., Sharp, W.D., Zhang, P.Z., 2006b. East Asian summer
552 monsoon variability during Marine Isotope Stage 5 based on speleothem $\delta^{18}\text{O}$
553 records from Wanxiang Cave, central China, *Palaeogeogr. Palaeoclimatol.*
554 *Palaeoecol.*, 236, 2-19.
555

556 Joussaume, S., Taylor, K.E., 1995. Status of the Paleoclimate Modeling Intercomparison
557 Project (PMIP), in Proceedings of the first international AMIP scientific
558 conference, WCRP Report, 425-430.
559

560 Kalnay, E., et al., 1996. The NCEP/NCAR 40-Year Reanalysis Project, *Bull. Am.*
561 *Meteorol. Soc.*, 77, 437-472.
562

563 Kelly, M. J., Edwards, R.L., Cheng, H., Yuan, D., Cai, Y., Zhang, M., Lin, Y., An, Z.,
564 2006. High resolution characterization of the Asian Monsoon between 146,000
565 and 99,000 years B.P. from Dongge Cave and global correlation of events
566 surrounding Termination II, *Palaeogeogr. Palaeoclimatol. Palaeoecol.*, 236, 20-38.
567

568 Kutzbach, J.E., 1981. Monsoon climate of the early Holocene: Climate experiment with
569 the earth's orbital parameters for 9000 years ago, *Science*, 214, 59-61.
570

571 Lee, E., Chase, T.N., Rajagopalan, B., 2008. Seasonal forecasting of East Asian summer
572 monsoon based on oceanic heat sources, *Int. J. Climatol.*, 28, 667-678.
573

574 Lee, J.-E., Fung, I., DePaolo, D.J., Henning, C.C., 2007. Analysis of the global
575 distribution of water isotopes using the NCAR atmospheric general circulation
576 model, *J. Geophys. Res.*, 112, doi:10.1029/2006JD007657.
577

578 Lee, J.-E., Fung, I., 2008. "Amount effect" of water isotopes and quantitative analysis of
579 post-condensation processes, *Hydrol. Process.*, 22, 1-8.
580

581 Legates, D.R., Willmott, C.J., 1990. Mean seasonal and spatial variability in gauge-
582 corrected, global precipitation, *Int. J. Climatol.*, 10, 111-127.
583

584 Maher, B., 2008. Holocene variability of the East Asian summer monsoon from Chinese
585 cave records: a re-assessment, *The Holocene*, 18, 861-866.
586

587 Risi, C., Bony, S., Vimeux, F., 2008. Influence of convective processes on the isotopic
588 composition ($\delta^{18}\text{O}$ and δD) of precipitation and water vapor in the tropics: 2.
589 Physical interpretation of the amount effect, *J. Geophys. Res.*, 113,
590 doi:10.1029/2008JD009943.
591

592 Rozanski, K., Araguás- Araguás, L., Gonfiantini, R., 1992. Relation between long-term
593 trends of oxygen-18 isotope composition of precipitation and climate, *Science*,
594 258, 981-985.
595

596 Sinha, A., Cannariato, K.G., Stott, L.D., Cheng, H., Edwards, R.L., Yadava, M.G.,
597 Ramesh, R., Singh, I.B., 2007. A 900-year (600 to 1500 A.D.) record of the
598 Indian summer monsoon precipitation from the core monsoon zone of India,
599 *Geophys. Res. Lett.*, 34, doi:10.1029/2007GL030431.
600

601 Vaks, A., Bar-Matthews, M., Ayalon, A., Schilman, B., Gilmour, M., Hawkesworth, C.J.,
602 Frumkin, A., Kaufman, A., Matthews, A., 2003. Paleoclimate reconstruction
603 based on the timing of speleothem growth and oxygen and carbon isotope
604 composition in a cave located in the rain shadow in Israel, *Quaternary Research*,
605 59, 182-193.
606

607 Wang, B., Fan, Z., 1999. Choice of south Asian summer monsoon indices, *Bull. Amer.*
608 *Metero. Soc.*, 80, 629-638.
609

610 Webster, P. J., Magaña, V.O., Palmer, T. N., Shukla, J., Tomas, R.A., Yanai, M.,
611 Yasunari, T., 1998. Monsoons: Processes, predictability, and the prospects for
612 prediction, *J. Geophys. Res.*, 103, 14,451-14,510.
613

614 Wang, Y. J., Cheng, H., Edwards, R.L., An, Z.S., Wu, J.Y., Shen, C.-C., Dorale, J. A.,
615 2001. A high-resolution absolute-dated late Pleistocene monsoon record from
616 Hulu Cave, China, *Science*, 294, 2345-2348.
617

618 Wang, Y.J., Cheng, H., Edwards, R.L., Kong, X.G., Shao, X.H., Chen, S.T., Wu, J.Y.,
619 Jiang, X.Y., Wang, X.F., An, Z.S., 2008. Millennial- and orbital-scale changes in
620 the East Asian monsoon over the past 224,000 years, *Nature*, 451, 1090-1093.
621

622 Yuan, D.X., Cheng, H., Edwards, R.L., Dykoski, C.A., Kelly, M.J., Zhang, M.L., Qing,
623 J.M., Lin, Y.S., Wang, Y.J., Wu, J.Y., Dorale, J.A., An, Z.S., Cai, Y.J., 2004.
624 Timing, duration and transition of the last interglacial Asian Monsoon, *Science*,
625 304, 575-578.
626

627 Zhou, Y, Gao, S., Shen, S.S.P., 2004. A diagnostic study of formation and structures of
628 the Meiyu Front System over East Asia, J. Meteor. Soc. Japan, 82, 1565-1576.
629

630 Table caption

631

632 Table 1: Correlation coefficients r and partial correlation coefficients ρ calculated from
633 nine GNIP stations for $\delta^{18}\text{O}$ values and precipitation P and temperature T . Sample size is
634 n . Coefficients that are significant at the 95% confidence interval are printed in bold
635 italics. A reduced degrees of freedom of $(n/3)-2$ is used in the monthly correlations to
636 account for autocorrelation in the records, which is significant for one or two month lags.

637

638

639 Figure captions

640

641 Figure 1: Elevation map of China and surrounding areas with locations of GNIP stations
642 used in this study. Dongge, Hulu, Heshang, and Xiaobailong cave locations are marked
643 with black dots. Insets show seasonal cycle of temperature (red lines, units of $^{\circ}\text{C}$, left
644 axis), precipitation (blue lines, units of cm/month , left axis), and $\delta^{18}\text{O}$ values (black lines,
645 units of ‰ , right axis). Dashed line indicates approximate northern limit of Meiyu front
646 (Zhou et al., 2004).

647

648 Figure 2: Annual mean (1920-1980) precipitation rate (mm/day) over southeast Asia
649 from the Legates Surface and Ship Observation of Precipitation dataset (Legates and
650 Willmott, 1990). Black contour lines denote elevations of 0 m and 2000 m. Note high
651 precipitation rates along the Himalayan front and in southeast China resulting from
652 Indian and East Asian monsoon activity.

653

654 Figure 3: Spatial correlation of annual mean precipitation (left) and temperature (right)
655 between a given site (top: Hulu cave, middle: Dongge cave, bottom: East India) and the
656 rest of Asia. Correlation coefficient is shown in filled contours, and correlations
657 significant at a 95% confidence interval are outlined by the black contour. Precipitation
658 and temperature from NCAR/NCEP Reanalysis (Kalnay et al. 1996).

659

660 Figure 4: Monthly total precipitation (mm , squares) and monthly mean temperature ($^{\circ}\text{C}$,
661 diamonds) versus monthly mean $\delta^{18}\text{O}$ values (‰) for stations at (a) Fuzhou, (b) Guilin,
662 (c) Guiyang, (d) Hong Kong, (e) Kunming, (f) Liuzhou, (g) Nanjing, (h) Shijiazhuang,
663 and (i) Zunyi. Linear regressions used in the calculations in the Discussion are shown in
664 black lines for stations at Guiyang, Hong Kong, Kunming, and Zunyi.

665

666 Figure 5: Annual average weighted $\delta^{18}\text{O}$ value relative to modern, D , as a function of (a)
667 f_o for $f' = 1$ and (b) f' for $f_o = 1$ calculated using equation (6) relative to modern values.
668 Dotted line (marked 'G') is calculation for station at Guiyang, dashed line (marked 'HK')
669 is Hong Kong, dot-dashed line (marked 'K') is Kunming, and solid line (marked 'Z') is
670 Zunyi. Values for a and P_o in equation (2) for the stations shown are: $a = -0.025$, $P_o =$
671 80.4 (Guiyang); $a = -0.0081$, $P_o = 196.1$ (Hong Kong); $a = -0.03$, $P_o = 83.0$ (Kunming);
672 and $a = -0.030$, $P_o = 81.5$ (Zunyi). Units of a and P_o are $\text{‰}/\text{mm}/\text{month}$ and mm/month ,
673 respectively.

674

Table 1: Correlation coefficients

station	monthly average			monthly anomaly			monthly average partial correlations		
	$r(\delta^{18}\text{O},\text{P})$	$r(\delta^{18}\text{O},\text{T})$	n	$r(\delta^{18}\text{O},\text{P})$	$r(\delta^{18}\text{O},\text{T})$	n	$\rho(\delta^{18}\text{O},\text{P},\text{T})$	$\rho(\delta^{18}\text{O},\text{T},\text{P})$	n
Fuzhou	-0.35	-0.38	71	-0.36	-0.08	71	-0.29	-0.33	71
Guilin	-0.20	-0.72	92	-0.18	0.00	92	0.09	-0.71	92
Guiyang	-0.48	-0.57	58	-0.31	0.11	58	-0.22	-0.40	58
Hong Kong	-0.61	-0.67	276	-0.33	-0.03	276	-0.36	-0.47	276
Kunming	-0.61	-0.44	152	-0.09	0.23	152	-0.48	-0.11	152
Liuzhou	-0.37	-0.55	45	-0.42	0.37	45	-0.27	-0.50	45
Nanjing	-0.45	-0.25	58	0.06	-0.07	58	-0.39	0.02	58
Shijiazhuang	-0.09	0.38	146	-0.20	0.30	146	-0.35	0.49	146
Zunyi	-0.56	-0.65	70	-0.34	0.07	70	-0.25	-0.44	70

Correlation coefficients that are significant at the 95% confidence level are shown in bold italics
degrees of freedom = $(n/3) - 2$

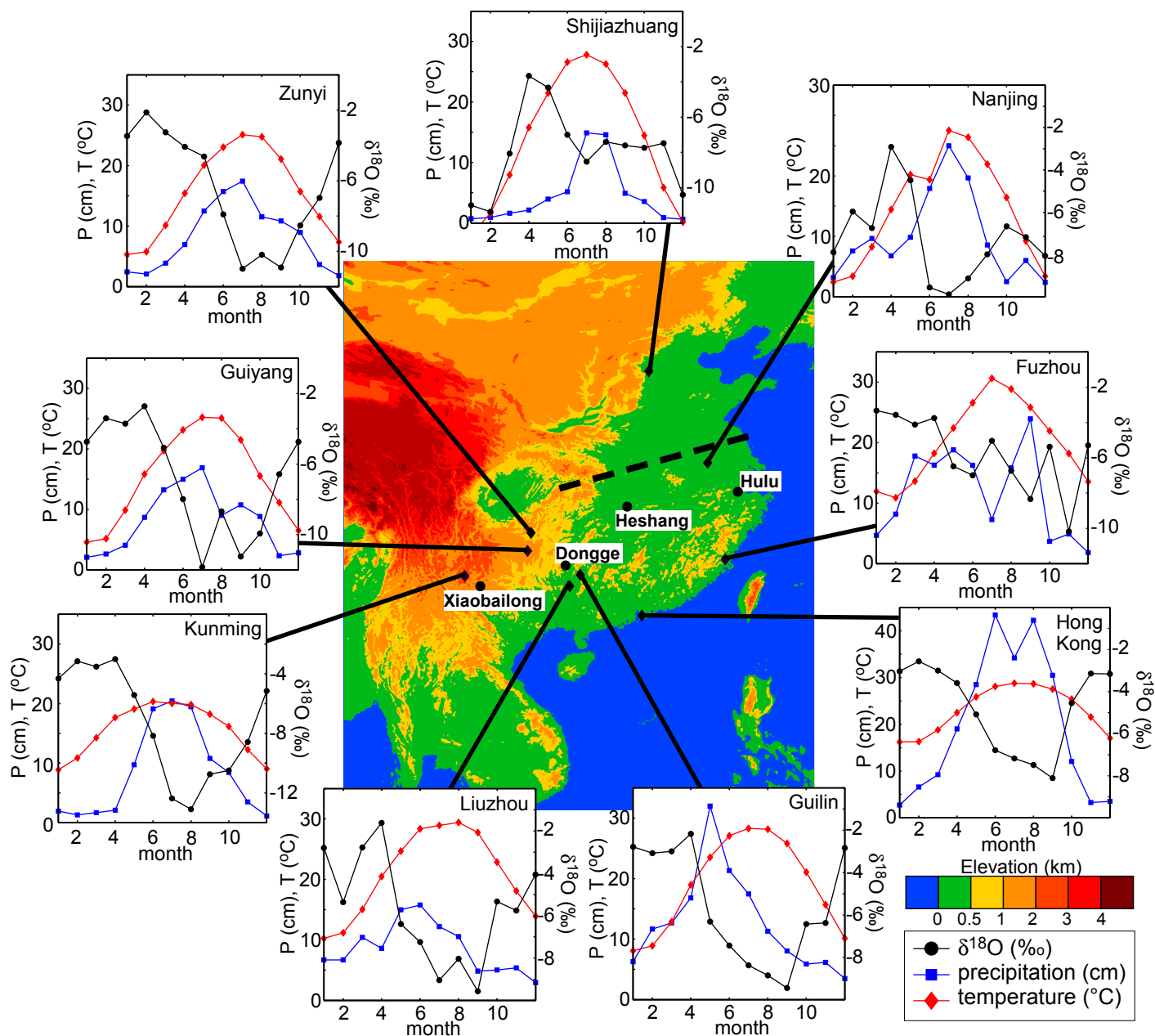


Figure 1: Elevation map of China and surrounding areas with locations of GNIP stations used in this study. Dongge, Hulu, Heshang, and Xiaobailong cave locations are marked with black dots. Insets show seasonal cycle of temperature T (red lines, units of $^{\circ}\text{C}$, left axis), precipitation P (blue lines, units of cm/month , left axis), and $\delta^{18}\text{O}$ values (black lines, units of ‰ , right axis). Dashed line indicates approximate northern limit of Meiyu front (Zhou *et al.*, 2004).

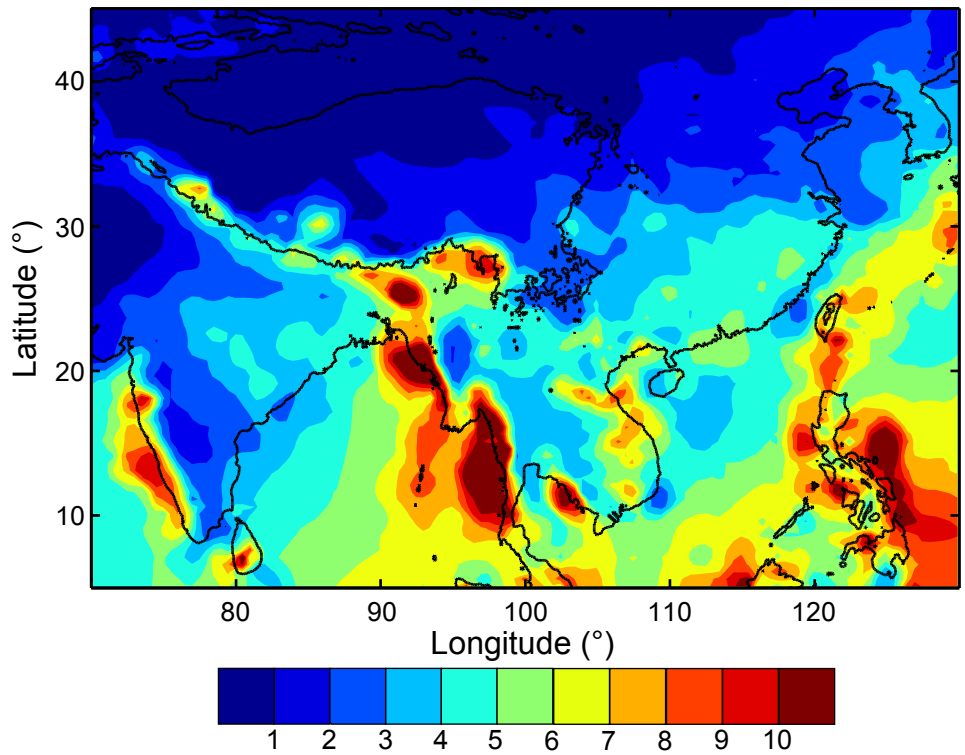


Figure 2: Annual mean (1920-1980) precipitation rate (mm/day) over southeast Asia from the Legates Surface and Ship Observation of Precipitation dataset (Legates and Willmott, 1990). Black contour lines denote elevations of 0 m and 2000 m. Note high precipitation rates along the Himalayan front and in southeast China resulting from Indian and East Asian monsoon activity.

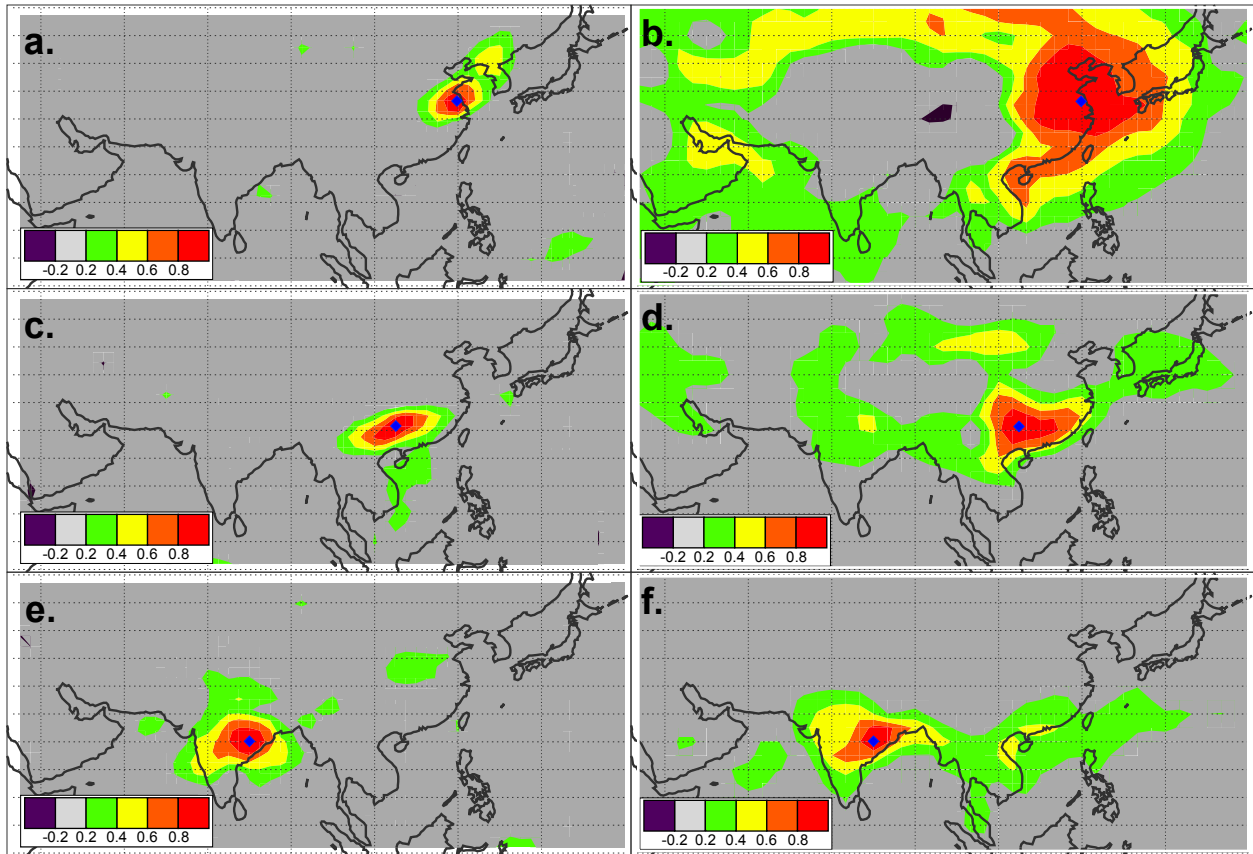


Figure 3: Spatial correlation of yearly average precipitation (left) and temperature (right) between a given site (top: Hulu cave, middle: Dongge cave, bottom: East India) and the rest of Asia. Correlation coefficient is shown in filled contours, and correlations significant at a 95% confidence interval are colored. Grey areas indicate insignificant correlations. Precipitation and temperature from NCAR/NCEP Reanalysis (Kalnay et al., 1996).

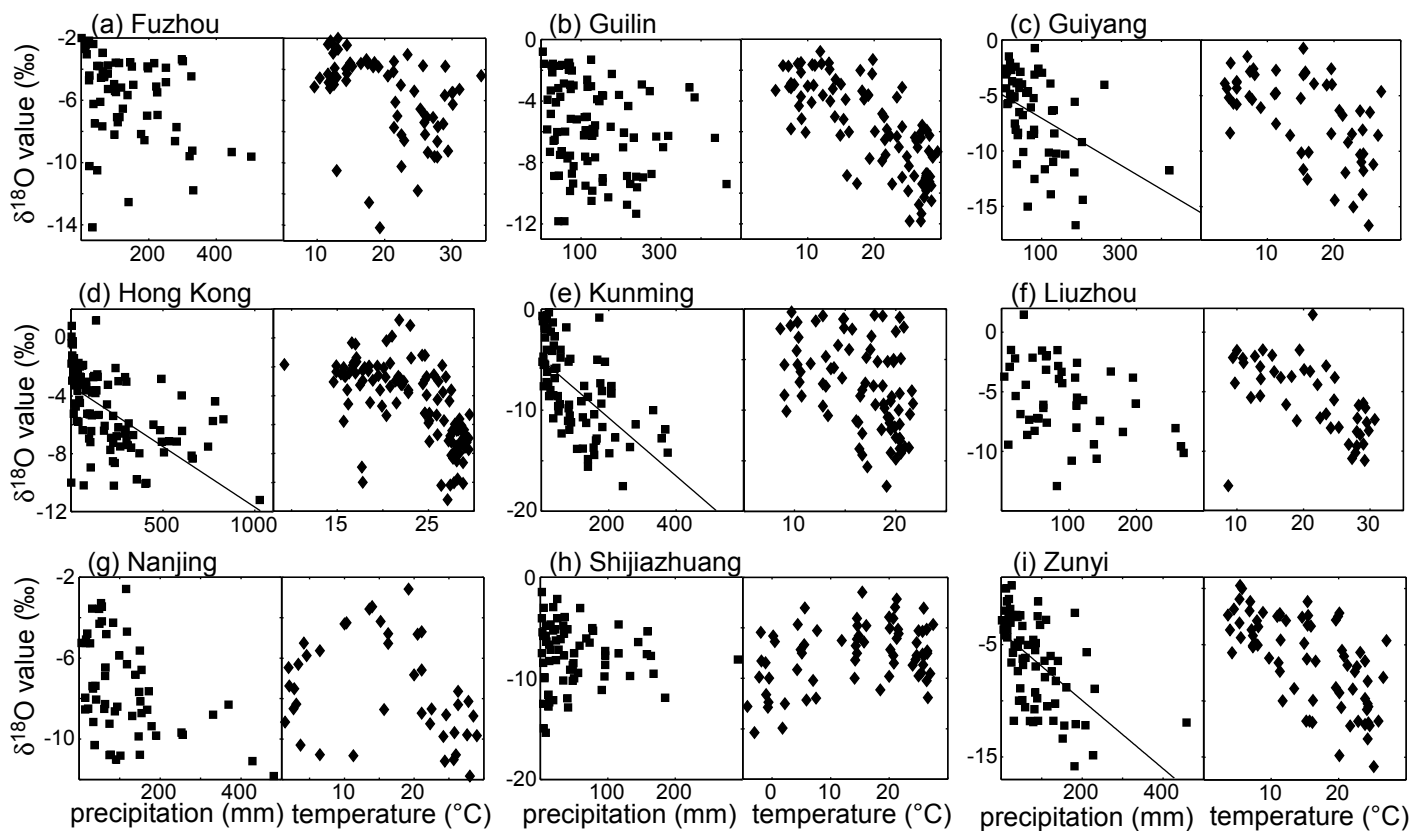


Figure 4: Monthly total precipitation (mm, squares) and monthly mean temperature (°C, diamonds) versus monthly mean $\delta^{18}\text{O}$ values (‰) for stations at (a) Fuzhou, (b) Guilin, (c) Guiyang, (d) Hong Kong, (e) Kunming, (f) Liuzhou, (g) Nanjing, (h) Shijiazhuang, and (i) Zunyi. Linear regressions used in the calculations in the Discussion are shown in black lines for stations at Guiyang, Hong Kong, Kunming, and Zunyi.

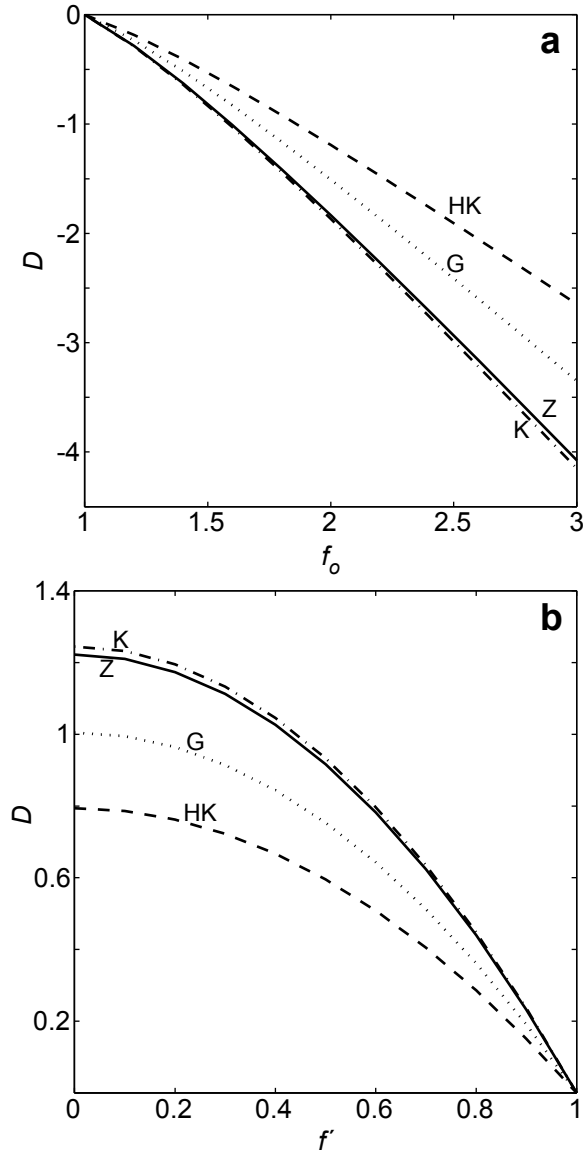


Figure 5: Annual average weighted $\delta^{18}\text{O}$ value relative to modern, D , as a function of (a) f_0 for $f' = 1$ and (b) f' for $f_0 = 1$ calculated using equation (6) relative to modern values. Dotted line (marked 'G') is calculation for station at Guiyang, dashed line (marked 'HK') is Hong Kong, dot-dashed line (marked 'K') is Kunming, and solid line (marked 'Z') is Zunyi. Values for a and P_0 in equation (2) for the stations shown are: $a = -0.025$, $P_0 = 80.4$ (Guiyang); $a = -0.0081$, $P_0 = 196.1$ (Hong Kong); $a = -0.03$, $P_0 = 83.0$ (Kunming); and $a = -0.030$, $P_0 = 81.5$ (Zunyi). Units of a and P_0 are $\text{‰}/\text{mm}/\text{month}$ and mm/month , respectively.